Inorganic Chemistry

pubs.acs.org/IC Article

Tuning the Separation of Light Lanthanides Using a Reverse-Size Selective Aqueous Complexant

Nikki A. Thiele, David J. Fiszbein, Joshua J. Woods, and Justin J. Wilson*

Cite This: *Inorg. Chem.* 2020, 59, 16522−16530 Read Online

ACCESS | Metrics & More | Article Recommendations | Supporting Information

ABSTRACT: Efficiently separating the chemically similar lanthanide ions into elementally pure compositions is one of the greatest scientific challenges of the 21st century. Although extensive research efforts have focused on the development of organic extractants for this purpose, the implementation of aqueous complexants possessing distinct coordination chemistries has scarcely been explored as an approach to enhancing intralanthanide separations. In this study, we investigate the lanthanide coordination chemistry of macrophosphi, a novel analogue of the reverse-size selective expanded macrocycle macropa. Our studies reveal that substitution of the pyridyl-2-carboxylic acid pendent arms of macropa with pyridyl-2-phosphinic acid arms of macrophosphi gives rise to a dramatic enhancement in the ability to discriminate between light lanthanides, reflected by a binding affinity of macrophosphi for La^{3+} that is over 5 orders of magnitude higher than that for Gd^{3+}. Furthermore, upon implementation of macrophosphi as an aqueous complexant in a biphasic extraction system containing the industrial extractant bis(2-ethylhexyl)phosphoric acid, separation factors of up to 45 were achieved for the Ce/La pair. These results represent a remarkable separation of adjacent lanthanides, demonstrating the significant potential of reverse-size selective aqueous complexants in lanthanide separation schemes.

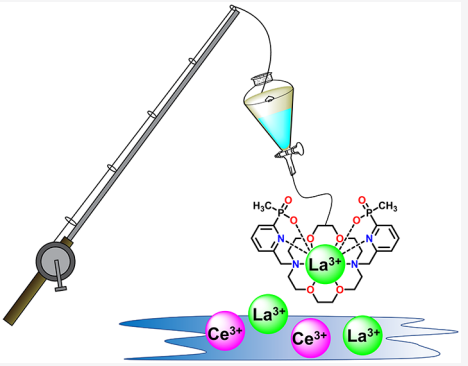

INTRODUCTION

The 15 lanthanides (Ln), comprising the elements lanthanum (La) through lutetium (Lu), exhibit a diverse range of photophysical, magnetic, and nuclear properties that render them uniquely suited for use in a wide range of applications spanning technology, industry, and medicine.[1] They are employed, for example, as key components of batteries and permanent magnets for hybrid vehicles and wind turbines, fluid cracking catalysts for gas production, and imaging and therapeutic agents for cancer diagnosis and treatment. Recently, the increasing demand for lanthanides for these applications, in conjunction with their tenuous supply arising from China's near monopoly on Ln production, has led to growing concern over the availability of these valuable elements to meet future needs.[2−4] This concern has prompted the designation of lanthanides as critical materials,[5,6] spurring innovative research into more efficient strategies for their recovery from mineral ores and secondary resources such as spent technology.[7−17] Owing to the similar chemical properties of the lanthanides,[18] however, their separation from one another into elementally pure streams, which is required for use in their respective applications, remains notoriously difficult.

The primary method by which lanthanides are separated from one another is liquid−liquid, or solvent, extraction.[19−21] In this process, an aqueous mixture of lanthanides is contacted with an immiscible organic solvent containing a lipophilic extractant such as bis(2-ethylhexyl)phosphoric acid (HDEHP; Figure 1), which serves to complex the lanthanides and transfer them into the organic phase.[22,23] The extent of partitioning of lanthanides between the two phases is based on the differential thermodynamic affinity of HDEHP for different Ln^{3+} ions. Like most ligands, HDEHP binds more strongly to the smaller heavy Ln^{3+} ions compared to the larger light Ln^{3+} ions and therefore is broadly effective at separating these two classes of lanthanides. Further tuning of separations may also be achieved by introducing a water-soluble complexant into the aqueous phase. In this context, the most commonly used aqueous complexant is diethylenetriaminepentaacetic acid (DTPA; Figure 1), which has been employed in the TALSPEAK (Trivalent Actinide−Lanthanide Separation by Phosphorus reagent Extraction from Aqueous Komplexes) separation process.[24,25] Like HDEHP, however, DTPA also has a strong binding preference for the smaller Ln^{3+} ions, with little ability to discriminate between neighboring or individual Ln^{3+} ions.[26] This redundancy with respect to metal-binding

Received: August 12, 2020
Published: October 24, 2020

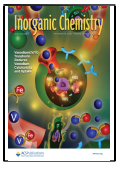

https://dx.doi.org/10.1021/acs.inorgchem.0c02413
Inorg. Chem. 2020, 59, 16522−16530

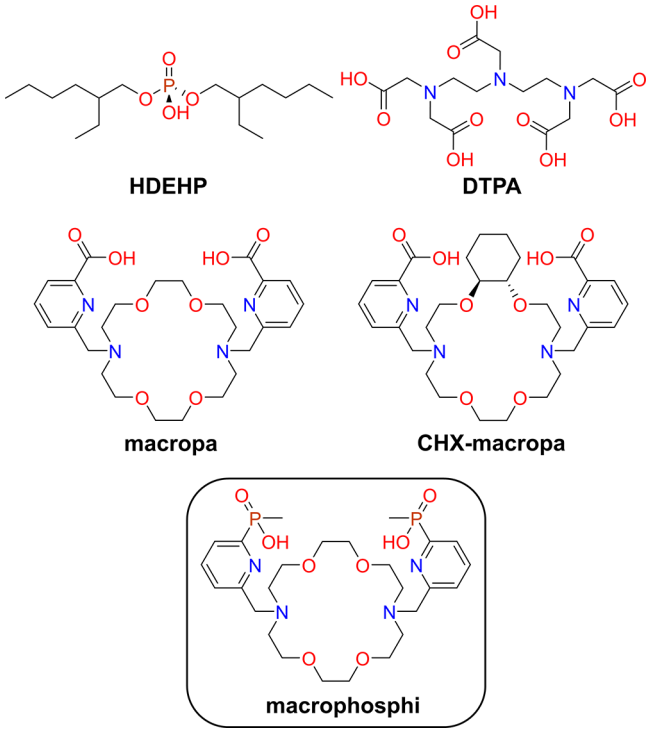

Figure 1. Chemical structures of the ligands discussed in this work.

preference currently limits the utility of these aqueous complexants in Ln separation schemes. Thus, the development of alternative aqueous complexants with Ln^{3+}-selectivity patterns distinct from those of the organic extractant is of great value to achieve more efficient Ln separations.

Although most ligands bind more strongly to the smaller, more charge-dense Ln^{3+} ions, there have been ongoing efforts to design ligands that have higher affinity for the larger, more charge-diffuse Ln^{3+} ions.[27−33] These "reverse-size" selective ligands have marked potential for use as aqueous complexants in liquid−liquid extractions in conjunction with conventional organic extractants. Efforts to implement these ligands in Ln separation schemes, however, have only been scarcely pursued. For example, the expanded 18-membered macrocyclic ligand macropa (Figure 1), a well-known reverse-size selective ligand,[33−35] has been applied in Ln and actinide (An) liquid−liquid extractions.[36,37] These studies have shown promising results, with macropa giving rise to a trans-lanthanide (Lu/La) separation factor (SF) of 10^8 and an average intralanthanide SF of 3.7 when used in a biphasic system with HDEHP.

Recently, our group has been developing new analogues of macropa for various applications in medicine and industry that require the selective chelation of large metal ions.[38−42] We have found that subtle modifications to the core scaffold can be made to tune the relative affinities of the resulting ligands for the different Ln^{3+} ions but preserve the overall trend of reverse-size selectivity. For example, a rigidified version of macropa, called CHX-macropa (Figure 1), exhibits an enhanced difference in binding affinity between La^{3+} and Lu^{3+} in comparison to macropa.[40] In this report, we describe a new diaza-18-crown-6 analogue called macrophosphi, in which the pyridyl-2-carboxylic acid (picolinic acid) pendent arms of macropa are replaced with pyridyl-2-phosphinic acid arms. We show that this modification leads to an augmented ability to discriminate between the early, but not late, Ln^{3+} ions, a feature that is distinct from that of macropa. With this unusual Ln^{3+}-selectivity pattern, macrophosphi was applied as an aqueous complexant in liquid−liquid Ln separation experiments. The use of this ligand has allowed us to demonstrate one of the largest SFs for adjacent Ln^{3+} ions reported to date. Collectively, these results highlight the utility of reverse-size selective aqueous complexants in the recovery of lanthanides and represent a significant advancement toward achieving the elusive goal of separating adjacent lanthanides in a single stage.

RESULTS AND DISCUSSION

Ligand Synthesis and Characterization. The synthesis of macrophosphi, a diaza-18-crown-6 macrocycle bearing two pyridyl-2-phosphinic acid pendent arms, was achieved in four steps (Scheme 1). A key challenge in preparing this ligand was the synthesis of the pendent arm synthon ethyl [6-

Scheme 1. Synthesis of Macrophosphi

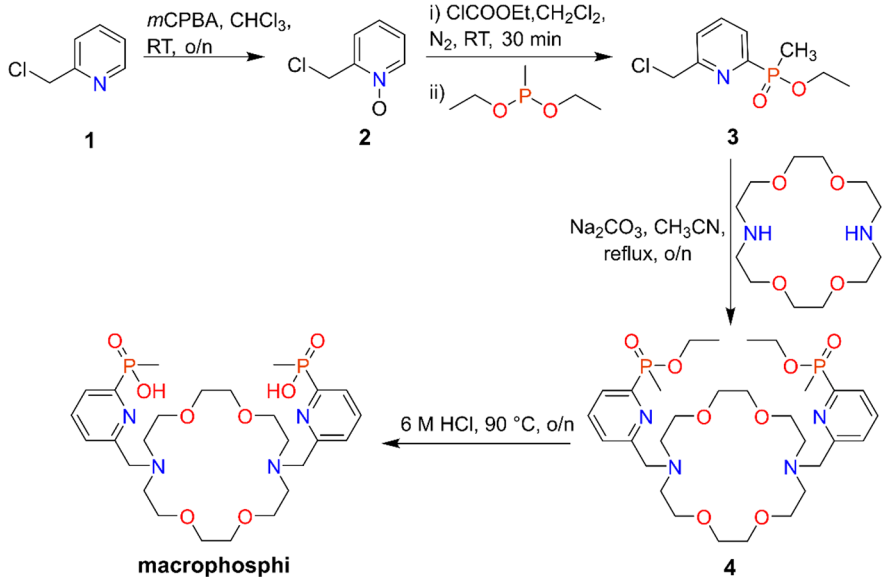

https://dx.doi.org/10.1021/acs.inorgchem.0c02413
Inorg. Chem. 2020, 59, 16522−16530

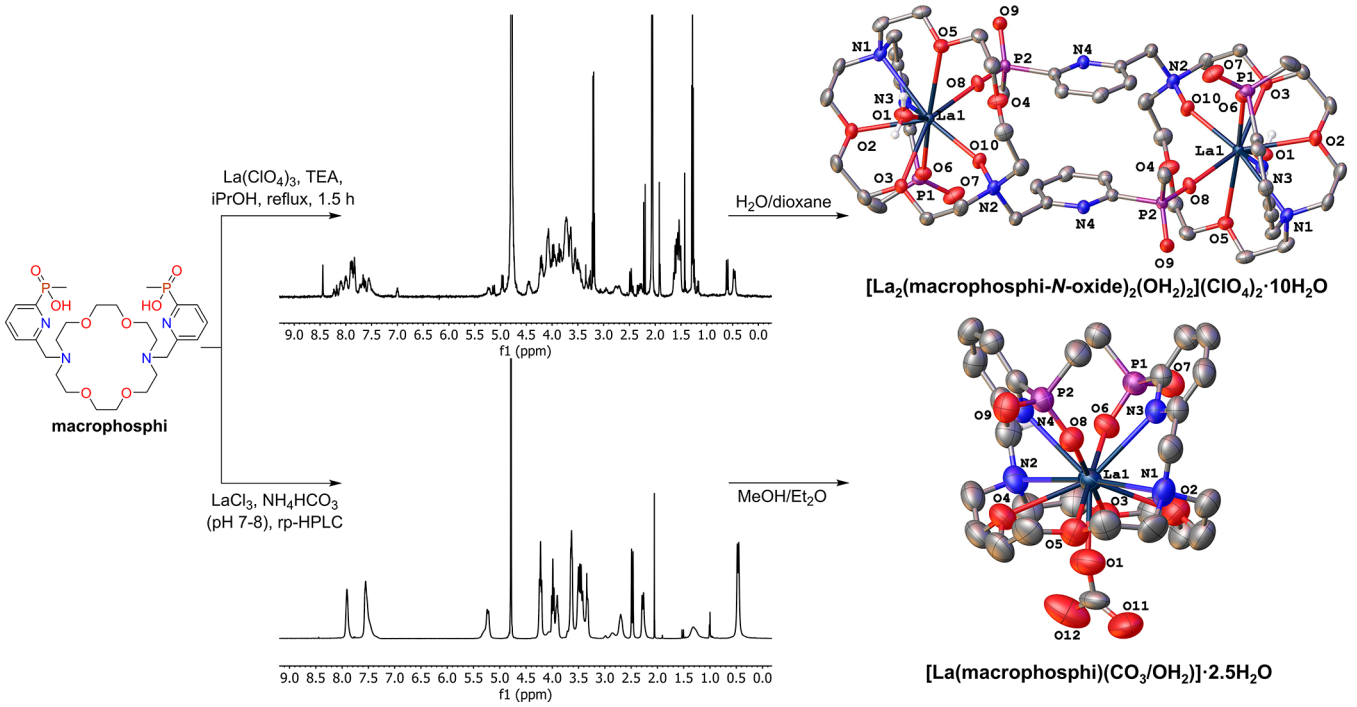

Figure 2. Synthesis and crystallization of La^{3+} complexes of macrophosphi. Top: ^{1}H NMR spectrum of the precipitate isolated from the reaction of macrophosphi with $La(ClO_4)_3$ in an organic solvent and X-ray crystal structure of the *N*-oxide dimer $[La_2(macrophosphi\text{-}N\text{-}oxide)_2(OH_2)_2](ClO_4)_2 \cdot 10H_2O$ obtained from crystallization of this precipitate from water/dioxane. Bottom: ^{1}H NMR spectrum of the precipitate isolated from the reaction of macrophosphi with $LaCl_3$ in aqueous NH_4HCO_3 and X-ray crystal structure of the monomeric, unoxidized complex $[(La\text{—}macrophosphi)(CO_3/OH_2)] \cdot 2.5H_2O$ obtained from crystallization of this precipitate from $MeOH/Et_2O$. The structure is shown here with the CO_3^{2-} anion occupying the axial position (see the text). Ellipsoids are drawn at the 50% probability level. Hydrogen atoms attached to carbon centers, counteranions, and outer-sphere water molecules are omitted for clarity.

(chloromethyl)pyridin-2-yl](methyl)phosphinate (**3**). Although compound **3** has not been previously reported, a closely related mesylate analogue has been prepared in five steps starting from 2-bromo-6-methylpyridine.[43,44] A key step in this synthesis is a palladium-catalyzed cross-coupling reaction to form the C—P bond, which requires rigorous anhydrous and oxygen-free conditions. In our approach, we employed a more straightforward synthetic route, requiring fewer steps and less sensitive reactions.

Our synthesis of **3** commenced from 2-(chloromethyl)-pyridine-1-oxide (**2**), which can be prepared on a multigram scale in high yield by treating 2-(chloromethyl)pyridine with *m*-chloroperoxybenzoic acid (mCPBA).[45] In the key C—P bond-forming step of our synthesis, the pyridine-*N*-oxide **2** was activated toward an Arbuzov-type reaction with ethyl chloroformate and then treated in the same pot with diethyl methylphosphonite to install the phosphinate group, protected as an ethyl ester. In contrast to the palladium-catalyzed C—P bond formation, no rigorous drying or degassing of the reaction mixture was required; only a sieve-dried solvent and a blanket of N_2 were used to exclude excessive moisture from the reaction. Compound **3** was isolated in 40—50% yield after vacuum distillation and subsequent flash column chromatography. Although this modified Arbuzov reaction is well established for the synthesis of pyridyl 2-phosphonates,[46,47] to the best of our knowledge, this report is the first example of its use to access the pyridyl-2-phosphinate scaffold. We anticipate that this alternate synthetic route to form pyridyl-2-phosphinates, which only requires two steps, will facilitate the implementation of this underutilized bidentate chelating moiety in future ligand design efforts.

Subsequent alkylation of diaza-18-crown-6 with **3** in acetonitrile at reflux resulted in the formation of **4** as a single diastereomer in approximately 63% yield (Scheme 1). Following purification of **4** by reverse-phase semipreparative high-performance liquid chromatography (rp-HPLC), the ester groups were hydrolyzed in 6 M HCl to afford macrophosphi as a crystalline hydrochloride salt (81% yield). Novel compounds **3**, **4**, and macrophosphi were fully characterized by ^{1}H, $^{13}C\{^{1}H\}$, and $^{31}P\{^{1}H\}$ NMR spectroscopy, analytical HPLC, high-resolution mass spectrometry (HRMS), and elemental analysis (Figures S1—S15).

The crystal structure of macrophosphi was determined by X-ray diffraction of a single crystal grown from slow evaporation of a methanol (MeOH) solution of the ligand (Figure S16). Under these conditions, macrophosphi crystallizes in the $P\bar{1}$ space group as a dihydrochloride salt, $[H_4macrophosphi]Cl_2$. The macrocycle sits on a crystallographic inversion center, and several regions of the structure exhibit disorder, reflecting some conformational flexibility of this compound (see section 1.2 in the SI for more details). The pendent arms are positioned above and below the plane of the macrocycle, with the pyridyl-2-phosphinate groups pointing away from the center of the diaza-18-crown-6 core. Crystallographic parameters for $[H_4macrophosphi]Cl_2$ are provided in Table S1.

Solution and Solid-State Characterization of La^{3+} Complexes of Macrophosphi. To probe the Ln coordination chemistry of macrophosphi, we first investigated its complexation with La^{3+}, the largest Ln^{3+} ion. Initial efforts to synthesize the La—macrophosphi complex were carried out in isopropyl alcohol using $La(ClO_4)_3$ as the La^{3+} source and triethylamine as a base (Procedure 1 in section 1.1 in the SI).

https://dx.doi.org/10.1021/acs.inorgchem.0c02413
Inorg. Chem. 2020, 59, 16522—16530

We have previously demonstrated that these reaction conditions are suitable to obtain Ln and alkaline-earth complexes of macropa.[38,39] The white precipitate isolated from this reaction was poorly soluble in all common NMR solvents, including DMSO-d_6, CD_3OD, and $CDCl_3$. Analysis of a slightly more soluble solution of the complex in D_2O by ^1H (Figures 2, top, and S17) and $^{31}P\{^1H\}$ (Figure S18) NMR spectroscopy revealed the presence of multiple species. Although the identities of these species could not be conclusively verified from this spectrum, several of these resonances were suggestive of La−macrophosphi complex formation (vide infra).

Single crystals suitable for X-ray diffraction were subsequently obtained via slow evaporation of an aqueous solution of the isolated powder within a closed vial of 1,4-dioxane after 7 months. Surprisingly, the crystal structure revealed a La_2L_2 dimer, where each half of the dimer is related by a crystallographic inversion center. In this structure, only one of the pyridyl-2-phosphinate pendent arms of macrophosphi binds to the La^{3+} center along with the other donors of the macrocycle. The other pyridyl-2-phosphinate pendent arm acts as a bridging ligand by binding to an adjacent La^{3+} center (Figure 2, top). Additionally, significant residual electron density was located between the La^{3+} center and the tertiary macrocyclic nitrogen atom bearing the bridging pendent arm. On the basis of the magnitude of this electron density, it was modeled as an oxygen atom. The distance between the tertiary nitrogen atom and this oxygen atom refined to a value of 1.371 Å, which is consistent with other N−O distances within *N*-oxide functional groups.[48] Furthermore, HRMS analysis of the crystals shows molecular-ion peaks that reflect the presence of an additional oxygen atom in these macrocycles, providing further support for our assignment (Figure S19). Although these data conclusively demonstrate that one diaza crown nitrogen atom of each macrophosphi ligand in the dimer is oxidized, it is unclear whether oxidation occurred during the synthesis of the complex or over the course of its crystallization.

Further analysis of this structure shows that the La^{3+} centers are 9-coordinate, with an N_2O_7 coordination sphere that is provided by the *N*-oxide oxygen atom, three ether oxygen atoms and the unoxidized nitrogen atom of the macrocycle, two deprotonated phosphinate oxygen atoms, one pyridyl nitrogen atom, and one inner-sphere water molecule. As noted above, one of the two coordinated phosphinate oxygen atoms (O8) originates from the adjacent ligand in the dimer. The pyridyl nitrogen atoms (N4) of the bridging pyridyl-2-phosphinate groups do not engage in metal coordination. Additionally, one ether oxygen atom of the macrocycle (O4) is omitted from our consideration of the coordination environment of the complex because of the large La1−O4 interatomic distance of 3.267 Å, which precludes any significant interaction between these two atoms. Two disordered perchlorate counteranions balance the charge of the 2+ dimer, and 10 molecules of water are present in the outer coordination sphere, giving rise to a complex of the formula $[La_2(\text{macrophosphi-}N\text{-oxide})_2(OH_2)_2](ClO_4)_2\cdot 10H_2O$ (Table S1).

The unexpected dimeric crystals of the La^{3+}−macrophosphi complex prompted us to find alternative synthetic and crystallization methods to obtain the intended 1:1 complex. The successful synthesis of the monomeric unoxidized La−macrophosphi complex was achieved in aqueous solution by mixing $LaCl_3$ and macrophosphi in a NH_4HCO_3 buffer at pH 7−8 (Procedure 2 in section 1.1 in the SI). The resulting complex was purified by rp-HPLC using an NH_4HCO_3-buffered mobile phase, followed by lyophilization to afford a white powder. Analysis of the isolated powder by ^1H, $^{13}C\{^1H\}$, and $^{31}P\{^1H\}$ NMR spectroscopy (Figures 2, bottom, and S20−S25) and HRMS (Figure S26) reveals the presence of key spectroscopic signatures of the monomeric complex. However, two species are detected by NMR spectroscopy and are presumed to be different diastereomeric forms of the complex. For example, two distinct signals are observed for the phosphinate CH_3 groups, with one signal appearing as a sharp doublet at 0.46 ppm and the other as a broad singlet at 1.32 ppm. These two diastereomers arise from coordination of the phosphinate group to the metal center, which gives rise to chirality (*R* or *S*) at the phosphorus center. Notably, upon heating of the sample to 80 °C, all of the peaks sharpen and coalesce, indicating that fast interconversion between diastereomers occurs at this temperature (Figures S21 and S25). This observation is consistent with the phosphorus atom chirality being enforced by metal coordination because higher temperatures will increase the on−off rate of these pendent donors, enabling them to racemize. At 80 °C, the NMR spectra show a single set of signals that reflect an effective C_2 symmetry of the complex in solution, providing further support for the fact that this complex exists as a simple monomeric species in solution. Also noteworthy in the $^{13}C\{^1H\}$ NMR spectrum of the complex at 80 °C is the presence of a resonance at 160.57 ppm (Figure S22). The chemical shift of the signal matches that of $NaHCO_3$ in D_2O (Figures S27 and S28), suggesting that the isolated complex contains the HCO_3^- anion. This finding is consistent with the use of aqueous NH_4HCO_3 in its synthesis and indicates that this species may be a counterion of the La−macrophosphi complex.

The solid-state structure of monomeric La−macrophosphi was obtained by X-ray diffraction of a single crystal grown from the vapor diffusion of diethyl ether (Et_2O) into a MeOH solution of the complex (Figure 2, bottom). In this structure, the La^{3+} ion is coordinated by all 10 donor atoms of the ligand, with both pyridyl-2-phosphinate arms oriented in a syn conformation above the plane of the macrocycle. Additionally, residual electron density was found at the axial coordination site of the metal center. This feature was also observed in the crystal structure of the La^{3+} complex of macropa, which showed that a water molecule coordinated from below the macrocycle.[38] In the case of La−macrophosphi, the arrangement of the electron density looked like a trigonal-planar CO_3^{2-} anion. Its magnitude, however, was too low to be satisfactorily modeled as such. Only the electron density directly coordinated to the La center could be refined as a full-occupancy oxygen atom. However, refinement of the other atoms in 50% occupancy was satisfactory. As such, we tentatively assigned this structure as [La(macrophosphi)-(OH_2)]/[La(macrophosphi)(CO_3)] with disorder over the axial water and carbonate positions. This assignment gives a satisfactory charge balance within the crystal, with the 1+ charge of the water complex complementing the 1− charge of the CO_3^{2-} complex. However, it also precludes confidence in the axial La−O interatomic distances. A detailed discussion of the refinement procedure can be found in section 1.2 in the SI. Crystallographic parameters for [La(macrophosphi)$(CO_3/OH_2)]\cdot 2.5H_2O$ are provided in Table S1.

https://dx.doi.org/10.1021/acs.inorgchem.0c02413
Inorg. Chem. 2020, 59, 16522−16530

Macrophosphi can adopt several different conformations upon binding to a metal ion. Its absolute configuration in a complex can be assigned using *R* or *S* to denote the chirality of each of the two phosphorus atoms of the pyridyl-2-phosphinate arms, Δ or Λ to designate the direction of the pendent arm helical twist, and δ or λ to indicate the tilt of each five-membered chelate ring.[49] In the crystal structure of [La(macrophosphi)(CO_3/OH_2)]·2.5H_2O, the ligand attains the conformation *SS*-Δ($\delta\lambda\delta$)($\delta\lambda\delta$), present in an amount equal to that of its enantiomer *RR*-Λ($\lambda\delta\lambda$)($\lambda\delta\lambda$). Notably, the Δ($\delta\lambda\delta$)($\delta\lambda\delta$) conformation is also observed for macropa complexed with La^{3+} and other large metal ions,[35,38,39] suggesting that changing the pendent arms from pyridyl-2-carboxylate to pyridyl-2-phosphinate groups does not impact the preferred configuration of the ligand. The metal−ligand interatomic distances for [La(macrophosphi)(CO_3/OH_2)], however, vary significantly in comparison to those of [La(macropa)(OH_2)]$^+$. For example, the interatomic distances between the La center and ether oxygen atoms of the macrocycle (O2−5) are, on average, 0.13 Å longer in the macrophosphi complex. In addition, the interatomic distances between La and the phosphinate oxygen atoms (O6 and O8) are approximately 0.13 Å shorter compared to those between La and the picolinate oxygen atoms in the macropa complex. Furthermore, the interatomic distances between the La center and the pyridyl nitrogen atoms of macrophosphi are approximately 0.08 Å longer than the corresponding distances in the La−macropa complex. Collectively, these results show that the overall conformation of [La(macrophosphi)(CO_3/OH_2)], Δ($\delta\lambda\delta$)($\delta\lambda\delta$), is the same as that of [La(macropa)(OH_2)]$^+$, but the actual interactions between the donor atoms, as reflected by interatomic distances, vary significantly by replacing the pyridyl-2-carboxylate arms of macropa with the pyridyl-2-phosphinate arms of macrophosphi.

Thermodynamic Solution Studies. To further investigate the impact of modifying the pendent arm donors appended to the diaza-18-crown-6 scaffold on the coordination properties of the ligand, we determined the protonation constants of macrophosphi and the pH-independent stability constants of its complexes with the Ln^{3+} series (except Pm^{3+}) by pH-potentiometric titration in 0.1 M KCl at 25 °C. To our knowledge, this is the first time that the thermodynamic binding constants of a chelator bearing the pyridyl-2-phosphinate group have been measured. The results are compiled in Table 1 and Figures S29−S31. For comparison, the protonation and stability constants for macropa[34] and CHX-macropa[40] are also provided. From potentiometric titrations of macrophosphi in the absence of metal ions, three ligand protonation constants (log K_{ai}; eq 1) were determined. The first two protonation constants of 8.13 (log K_{a1}) and 6.77 (log K_{a2}) are assigned to the amine nitrogen atoms of the macrocycle. The third protonation constant, log K_{a3}, is assigned to the protonation of a phosphinate oxygen atom. Its value of 1.97 is substantially lower than the corresponding protonation constants assigned to the picolinate groups of macropa (3.32 and 2.36 for log K_{a3} and log K_{a4}, respectively). This lower value is expected based on the greater acidity of simple aminophosphinic acids compared to aminocarboxylic acids, which reflects the stronger electron-withdrawing properties of the $-P(CH_3)O_2^-$ group of pyridyl-2-phosphinate compared to the CO_2^- group of pyridyl-2-carboxylate.[50] The remaining three protonation constants of macrophosphi were too low to be accurately determined by potentiometric titration. Collectively, the overall basicity of macrophosphi, expressed as the sum of its three log K_{ai} values, is 16.87, which is 4.76 log units less than that of macropa and 3.53 log units less than that of CHX-macropa.

Table 1. Protonation Constants of Macrophosphi and Thermodynamic Stability Constants of Its Ln^{3+} Complexes Determined by pH Potentiometry (25 °C and *I* = 0.1 M KCl)[a]

	macrophosphi^{2-}	CHX-macropa^{2-}[b]	macropa^{2-}[c]
log K_{a1}	8.13(1)	7.77(1)	7.41
log K_{a2}	6.77(1)	6.95(1)	6.85
log K_{a3}	1.97(8)	3.17(4)	3.32
log K_{a4}		2.51(7)	2.36
log K_{a5}			1.69
log K_{LaL}	12.94(6)	14.54(1)	14.99
log K_{LaHL}			2.28
log K_{CeL}	11.92(3)	14.38(3)	15.11
log K_{CeHL}			2.07
log K_{PrL}	11.12(4)	13.89(1)	14.70
log K_{PrHL}			2.96
log K_{NdL}	10.44(6)	13.57(5)	14.36
log K_{NdHL}			2.08
log K_{SmL}	9.34(2)	12.79(1)	13.80
log K_{SmHL}			2.70
log K_{EuL}	8.68(2)	12.25(3)	13.01
log K_{EuHL}			1.97
log K_{GdL}	7.82(2)	11.53(2)	13.02
log K_{GdHL}			2.48
log K_{TbL}	7.24(3)	10.98(4)	11.79
log K_{TbHL}			2.91
log K_{DyL}	6.83(4)	10.34(3)	11.72
log K_{DyHL}			2.42
log K_{HoL}	6.69(3)	9.67(5)	10.59
log K_{ErL}	6.73(1)	8.96(6)	10.10
log K_{TmL}	6.76(2)	8.19(3)	9.59
log K_{YbL}	6.78(3)	7.44(4)	8.89
log K_{LuL}	6.67(3)	6.70(1)	8.25

[a]Data for CHX-macropa and macropa provided for comparison. [b]Reference 40. [c]Reference 34.

$$K_{ai} = \frac{[H_iL]}{[H_{i-1}L][H^+]} \quad (1)$$

$$K_{ML} = \frac{[ML]}{[M][L]} \quad (2)$$

$$K_{MH_nL} = \frac{[MH_nL]}{[MH_{n-1}L][H]} \quad (3)$$

Following the determination of the protonation constants of macrophosphi, the stability constants, or log K_{ML} values (eq 2), of its complexes with the Ln^{3+} ions were measured by carrying out potentiometric titrations in the presence of 1 equiv of La−Tb or 0.5 equiv of Dy−Lu. A ligand-to-metal ratio of 2:1 was used in titrations of macrophosphi containing Dy−Lu to suppress the formation of insoluble lanthanide hydroxide species under basic conditions. These species arise from displacement of the ligand in the Ln complex by hydroxide ions, which is thermodynamically favored in the presence of Ln−L complexes of low stability. Additionally, no log K_{MHL} values (eq 3) could be reasonably refined from our titration data with macrophosphi. This result contrasts that of macropa,

https://dx.doi.org/10.1021/acs.inorgchem.0c02413
Inorg. Chem. 2020, 59, 16522−16530

for which monoprotonated (MHL) complexes have been reported with the large Ln^{3+} ions.[34]

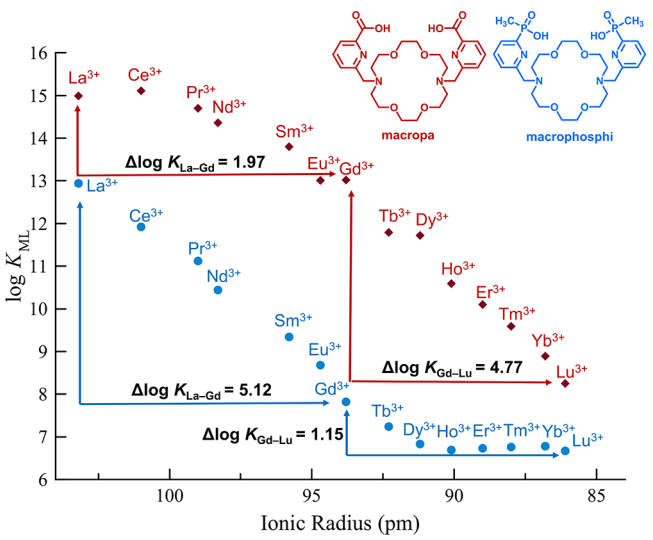

Figure 3. Comparison between the Ln stability constants (log K_{ML} values) of macrophosphi (blue circles) and macropa (red diamonds) as a function of the 6-coordinate ionic radius of each Ln^{3+} ion.

The smaller log K_{ML} values of macrophosphi across the entire Ln^{3+} series, as shown in Table 1 and Figure 3, indicate that this ligand forms complexes of lower thermodynamic stability in comparison to macropa and CHX-macropa. Generally, metal-ion affinity scales with the overall basicity of a ligand. This trend is apparent because the basicity can often be correlated to the ligand donor strength. Thus, the lower stability of Ln^{3+} complexes of macrophosphi was expected based on the lower basicity of macrophosphi in comparison to macropa and CHX-macropa. Despite this decrease in affinity for the lanthanides, macrophosphi retains reverse-size selectivity, showing a thermodynamic preference for large over small metal ions. Specifically, the difference in log K_{ML} values of La−macrophosphi and Lu−macrophosphi is 6.27, nearly identical to that of 6.74 for macropa. Thus, as expected, the diaza-18-crown-6 macrocycle maintains this unusual reverse-size selectivity pattern even in the presence of different pendent donors. Upon further analysis of the plot of log K_{ML} versus ionic radius, however, it is apparent that there are important differences in the selectivity patterns of macrophosphi and macropa (Figure 3). For the late Ln^{3+} ions (Gd−Lu), there is a span of 4.77 log K units for macropa but only 1.15 log K units for macrophosphi. By contrast, across the early Ln^{3+} ions (La−Gd), the log K_{ML} values of macrophosphi vary significantly (Δlog K = 5.12) but are relatively static for macropa (Δlog K = 1.95). These results show that more subtle trends and differences in thermodynamic stability of Ln^{3+} complexes manifest upon appropriate tuning of the pendent arm donors of this class of ligands. Furthermore, this observation is significant because it shows that these ligands, which are both reverse-size selective, would be optimally used for discriminating between different types of Ln^{3+} ions when employed for chemical separations.

Ln^{3+} Separation Using Liquid−Liquid Extraction. Following the thermodynamic stability studies described above, we sought to demonstrate the utility of macrophosphi as an aqueous complexant in liquid−liquid extraction schemes for the separation of light lanthanides. Extraction experiments were conducted at room temperature using an organic phase comprising HDEHP in *o*-xylene and an aqueous phase

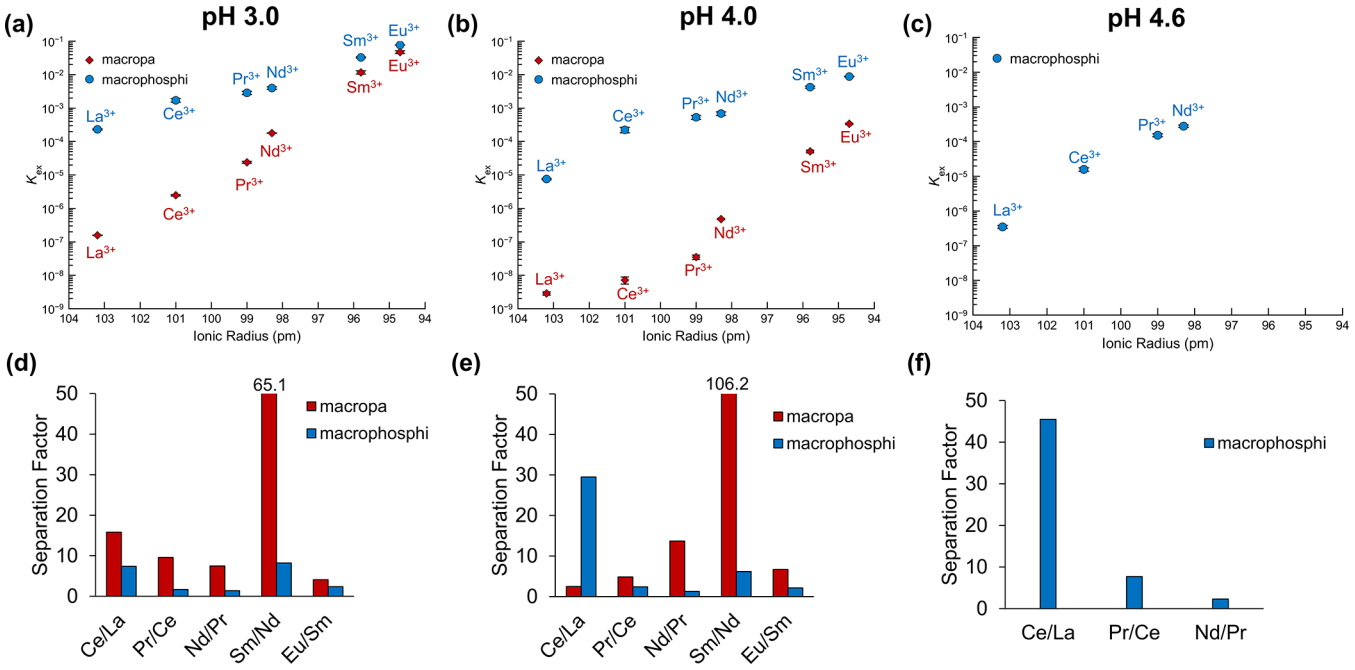

Figure 4. Equilibrium distribution of Ln^{3+} ions (La−Eu, excluding Pm) in a system comprising an organic phase of HDEHP in *o*-xylene and an aqueous phase of macrophosphi or macropa (1 mM) in 0.05 M sodium lactate/1 M $NaNO_3$ at various pH values. (a−c) Plots of conditional extraction constants (K_{ex}) as a function of the 6-coordinate ionic radius for liquid−liquid extractions carried out at pH 3.0, 4.0, and 4.6, respectively. (d−f) SFs for adjacent light Ln^{3+} pairs (except for Sm/Nd, which are separated by Pm) from liquid−liquid extractions carried out at pH 3.0, 4.0, and 4.6, respectively. Conditional extraction constants and SFs are defined in the main text.

https://dx.doi.org/10.1021/acs.inorgchem.0c02413
Inorg. Chem. 2020, 59, 16522−16530

comprising macrophosphi in 0.05 M sodium lactate/1 M $NaNO_3$ at equilibrium pH values of 3.0, 4.0, and 4.6. For comparison, extraction experiments at pH 3.0 and 4.0 were also carried out using macropa. This extraction using macropa at pH 3.0 was previously reported, and the values obtained in our study are consistent with this prior report, validating our experimental procedures (Figure S32).[36,37] The aqueous phase was loaded with a mixture of Ln^{3+} ions (0.01 mM each of La−Eu, excluding Pm), and the samples were rotated end over end for 24 h, unless otherwise noted. This period of time was found to be sufficient for samples to reach equilibrium, although extractions containing macropa were notably slower to reach equilibrium than those containing macrophosphi (Figures S33−S36). The equilibrium concentrations of Ln^{3+} ions in the aqueous phase of each sample were measured by inductively coupled plasma mass spectrometry (ICP-MS), and the Ln^{3+} distribution ratio (D_M), expressed as $[M]_{org}/[M]_{aq}$, was subsequently calculated from mass-balance equations. Because the stabilities of light lanthanide complexes of macrophosphi and macropa span several orders of magnitude, it was necessary to use a range of HDEHP concentrations in the organic phase to achieve measurable distributions for each Ln^{3+} ion. To account for this sample-to-sample variation in the HDEHP concentration, D_M values were normalized as described in section 1.4 in the SI to arrive at conditional extraction constants (K_{ex}), which can be directly compared across samples. These equilibrium constants scale with the concentration of the Ln^{3+} ion extracted into the organic phase by HDEHP, with larger values signifying greater transfer of Ln^{3+} ions into *o*-xylene than smaller values. From the ratio of K_{ex} values of two Ln^{3+} ions (K_{exLn1}/K_{exLn2}), the separation factor (SF) can be calculated. The SF is a measure of the selectivity of the system for one Ln^{3+} ion over another, reflecting the coordination chemistry of the aqueous complexant and nonaqueous extractant. All data from these experiments have been compiled in Tables S2−S14, and the results are summarized in Figure 4.

Moving across the lanthanide series from the large La^{3+} ion to the smaller Eu^{3+} ion, a monotonic increase is observed in the extraction of metal ions into *o*-xylene from the aqueous phase, irrespective of the pH or aqueous complexant (Figure 4a−c). This trend is expected based on the well-known preference of HDEHP for binding smaller over larger Ln^{3+} ions.[51] Additionally, the K_{ex} values for all Ln^{3+} ions studied are consistently smaller for extractions containing macropa versus those containing macrophosphi in the aqueous phase (Figure 4a−c), signifying a general reduction in partitioning of metal ions to the organic phase in macropa-containing systems. This trend arises from the overall higher thermodynamic affinity of macropa for all Ln^{3+} ions in comparison to macrophosphi (Table 1), which leads to their greater retention in the aqueous phase.

Upon closer inspection of the distribution plots, however, significant differences in the shapes of the extraction profiles of La^{3+}−Eu^{3+} can also be discerned between ligand systems as the pH is systematically altered. At pH 3, the K_{ex} values rise more sharply with decreasing ionic radius of the Ln^{3+} ion in the extraction system containing macropa than in the system containing macrophosphi (Figure 4a), indicating that the selective holdback of larger over smaller Ln^{3+} ions is enhanced for macropa over macrophosphi under these conditions. As such, larger SFs for adjacent Ln^{3+} ions are observed for macropa relative to macrophosphi at pH 3 (Figure 4d). For example, the Ce/La SF for an extraction containing macropa at pH 3 is 15.8, favoring La^{3+} over Ce^{3+} in the aqueous phase, whereas the Ce/La SF for an extraction containing macrophosphi is only 7.4. Upon increasing the pH of the aqueous phase to 4.0, however, a remarkable change in the extraction profiles occurs. At this pH, the K_{ex} values for the largest Ln^{3+} ions, La^{3+}, Ce^{3+}, and Pr^{3+}, are now fairly similar in the HDEHP/macropa system, but a significant increase in the slope of K_{ex} versus ionic radius is evident for these Ln^{3+} ions in the HDEHP/macrophosphi system (Figure 4b). Because of these changes, the SFs for adjacent Ln^{3+} pairs now increase as the ionic radii decrease in the HDEHP/macropa system, in contrast to our observations at pH 3.0. The SFs for adjacent Ln^{3+} ions in the HDEHP/macrophosphi system, however, are enhanced at this pH. Notably, the SF for the adjacent Ce/La pair approaches 30. This trend is further augmented by increasing the pH of the HDEHP/macrophosphi system to 4.6 (Figure 4c). At this pH, a SF of 45 for Ce/La is achieved (Figure 4f), representing the highest SF for an adjacent pair of Ln^{3+} ions reported to date in any separation scheme. Collectively, these results demonstrate the remarkable utility of macrophosphi as a reverse-size selective aqueous complexant in biphasic extractions for intralanthanide separations.

CONCLUSION

In summary, we have demonstrated that modifying the pendent arm donors of the diaza-18-crown-6 macrocyclic scaffold can subtly tune the Ln^{3+} coordination preferences of the ligand while maintaining reverse-size selectivity for large over small Ln^{3+} ions. Specifically, substitution of the pyridyl-2-carboxylate groups of macropa with the pyridyl-2-phosphinate groups of macrophosphi imparts a notable shift in intralanthanide selectivity, marked by a more pronounced thermodynamic discrimination between the light Ln^{3+} ions. Additionally, under conditions previously found effective for forming soluble Ln^{3+} complexes of macropa, we instead obtained a poorly soluble precipitate upon treating macrophosphi with La^{3+} in isopropyl alcohol, from which an *N*-oxide dimer was subsequently isolated by crystallization. These results further highlight the differences in coordination chemistry between these two ligands and present intriguing possibilities for the use of macrophosphi in solubility- and redox-based Ln separation schemes.[8,9,11,17] Finally, we applied macrophosphi as an aqueous complexant in the separation of Ln^{3+} ions by solvent extraction. Employing macrophosphi in conjunction with HDEHP, we achieved the highest SF reported to date for an adjacent pair of Ln^{3+} ions. The insight gained from this study is invaluable for guiding the development of more efficient separations of Ln^{3+} ions, demonstrating the remarkable potential of reverse-size selective aqueous complexants in liquid−liquid separation schemes. Furthermore, we have shown that subtle trends in the Ln^{3+} complex stabilities of new ligands can have significant ramifications on their implementation in chemical separations.

ASSOCIATED CONTENT

Supporting Information

The Supporting Information is available free of charge at https://pubs.acs.org/doi/10.1021/acs.inorgchem.0c02413.

Experimental details, compound characterization, and supporting figures and tables (PDF)

https://dx.doi.org/10.1021/acs.inorgchem.0c02413
Inorg. Chem. 2020, 59, 16522−16530

Accession Codes

CCDC 2020757−2020759 contain the supplementary crystallographic data for this paper. These data can be obtained free of charge via www.ccdc.cam.ac.uk/data_request/cif, or by emailing data_request@ccdc.cam.ac.uk, or by contacting The Cambridge Crystallographic Data Centre, 12 Union Road, Cambridge CB2 1EZ, UK; fax: +44 1223 336033.

AUTHOR INFORMATION

Corresponding Author

Justin J. Wilson − *Department of Chemistry and Chemical Biology, Cornell University, Ithaca, New York 14853, United States;* orcid.org/0000-0002-4086-7982; Email: jjw275@cornell.edu

Authors

Nikki A. Thiele − *Department of Chemistry and Chemical Biology, Cornell University, Ithaca, New York 14853, United States;* orcid.org/0000-0003-3301-0849

David J. Fiszbein − *Department of Chemistry and Chemical Biology, Cornell University, Ithaca, New York 14853, United States*

Joshua J. Woods − *Department of Chemistry and Chemical Biology and Robert F. Smith School for Chemical and Biomolecular Engineering, Cornell University, Ithaca, New York 14853, United States;* orcid.org/0000-0002-6213-4093

Complete contact information is available at: https://pubs.acs.org/10.1021/acs.inorgchem.0c02413

Author Contributions

The manuscript was written through contributions of all authors. All authors have given approval to the final version of the manuscript.

Notes

The authors declare no competing financial interest.

ACKNOWLEDGMENTS

This work was supported by funding from the College of Arts and Sciences at Cornell University and the Research Corporation for Science Advancement through a Cottrell Scholar Award to J.J.W. This research also made use of the NMR Facility at Cornell University, which is supported, in part, by the NSF under Award CHE-1531632. Prof. Louis A. Derry and Dr. Katherine Grant (Earth and Atmospheric Sciences, Cornell University) are thanked for assistance with ICP-MS measurements.

REFERENCES

(1) Cheisson, T.; Schelter, E. J. Rare Earth Elements: Mendeleev's Bane, Modern Marvels. *Science* **2019**, *363*, 489−493.

(2) Humphries, M. Rare Earth Elements: The Global Supply Chain. *Congressional Research Service Report for Congress*; Congressional Research Service: Washington, DC, 2012; R41347

(3) Nassar, N. T.; Du, X.; Graedel, T. E. Criticality of the Rare Earth Elements. *J. Ind. Ecol.* **2015**, *19*, 1044−1054.

(4) Eggert, R.; Wadia, C.; Anderson, C.; Bauer, D.; Fields, F.; Meinert, L.; Taylor, P. Rare Earths: Market Disruption, Innovation, and Global Supply Chains. *Annu. Rev. Environ. Resour.* **2016**, *41*, 199−222.

(5) Bauer, D.; Diamond, D.; Li, J.; Sandalow, D.; Telleen, P.; Wanner, B. *U.S. Department of Energy Critical Materials Strategy*; U.S. Department of Energy: Washington, DC, 2010.

(6) Bauer, D.; Diamond, D.; Li, J.; McKittrick, M.; Sandalow, D.; Telleen, P. *U.S. Department of Energy Critical Materials Strategy*; U.S. Department of Energy: Washington, DC, 2011.

(7) Zhao, X.; Wong, M.; Mao, C.; Trieu, T. X.; Zhang, J.; Feng, P.; Bu, X. Size-Selective Crystallization of Homochiral Camphorate Metal-Organic Frameworks for Lanthanide Separation. *J. Am. Chem. Soc.* **2014**, *136*, 12572−12575.

(8) Bogart, J. A.; Lippincott, C. A.; Carroll, P. J.; Schelter, E. J. An Operationally Simple Method for Separating the Rare-Earth Elements Neodymium and Dysprosium. *Angew. Chem., Int. Ed.* **2015**, *54*, 8222−8225.

(9) Bogart, J. A.; Cole, B. E.; Boreen, M. A.; Lippincott, C. A.; Manor, B. C.; Carroll, P. J.; Schelter, E. J. Accomplishing Simple, Solubility-Based Separations of Rare Earth Elements with Complexes Bearing Size-Sensitive Molecular Apertures. *Proc. Natl. Acad. Sci. U. S. A.* **2016**, *113*, 14887−14892.

(10) Yin, X.; Wang, Y.; Bai, X.; Wang, Y.; Chen, L.; Xiao, C.; Diwu, J.; Du, S.; Chai, Z.; Albrecht-Schmitt, T. E.; Wang, S. Rare Earth Separations by Selective Borate Crystallization. *Nat. Commun.* **2017**, *8*, 14438.

(11) Fang, H.; Cole, B. E.; Qiao, Y.; Bogart, J. A.; Cheisson, T.; Manor, B. C.; Carroll, P. J.; Schelter, E. J. Electro-Kinetic Separation of Rare Earth Elements Using a Redox-Active Ligand. *Angew. Chem., Int. Ed.* **2017**, *56*, 13450−13454.

(12) Li, X.-Z.; Zhou, L.-P.; Yan, L.-L.; Dong, Y.-M.; Bai, Z.-L.; Sun, X.-Q.; Diwu, J.; Wang, S.; Bünzli, J.-C.; Sun, Q.-F. A Supramolecular Lanthanide Separation Approach Based on Multivalent Cooperative Enhancement of Metal Ion Selectivity. *Nat. Commun.* **2018**, *9*, 547.

(13) Zhang, W.; Hietala, S.; Khriachtchev, L.; Hatanpää, T.; Doshi, B.; Koivula, R. Intralanthanide Separation on Layered Titanium(IV) Organophosphate Materials via a Selective Transmetalation Process. *ACS Appl. Mater. Interfaces* **2018**, *10*, 22083−22093.

(14) Healy, M. R.; Ivanov, A. S.; Karslyan, Y.; Bryantsev, V. S.; Moyer, B. A.; Jansone-Popova, S. Efficient Separation of Light Lanthanides(III) by Ligands with Tunable Rigidity. *Chem. - Eur. J.* **2019**, *25*, 6326−6331.

(15) Higgins, R. F.; Cheisson, T.; Cole, B. E.; Manor, B. C.; Carroll, P. J.; Schelter, E. J. Magnetic Field Directed Rare-Earth Separations. *Angew. Chem., Int. Ed.* **2020**, *59*, 1851−1856.

(16) Nelson, J. J. M.; Schelter, E. J. Sustainable Inorganic Chemistry: Metal Separations for Recycling. *Inorg. Chem.* **2019**, *58*, 979−990.

(17) Cole, B. E.; Cheisson, T.; Higgins, R. F.; Nakamaru-Ogiso, E.; Manor, B. C.; Carroll, P. J.; Schelter, E. J. Redox-Driven Chelation and Kinetic Separation of Select Rare Earths Using a Tripodal Nitroxide Proligand. *Inorg. Chem.* **2020**, *59*, 172−178.

(18) Cotton, S. Introduction to the Lanthanides. *Lanthanide and Actinide Chemistry*; John Wiley & Sons, Ltd., 2006; pp 1−7.

(19) Brown, C. G.; Sherrington, L. G. Solvent Extraction Used in Industrial Separation of Rare Earths. *J. Chem. Technol. Biotechnol.* **1979**, *29*, 193−209.

(20) Xie, F.; Zhang, T. A.; Dreisinger, D.; Doyle, F. A Critical Review on Solvent Extraction of Rare Earths from Aqueous Solutions. *Miner. Eng.* **2014**, *56*, 10−28.

(21) Wilson, A. M.; Bailey, P. J.; Tasker, P. A.; Turkington, J. R.; Grant, R. A.; Love, J. B. Solvent Extraction: The Coordination Chemistry behind Extractive Metallurgy. *Chem. Soc. Rev.* **2014**, *43*, 123−134.

(22) Otu, E. O.; Westland, A. D. Solvent Extraction with Organophosphonic Mono-Acidic Esters. *Solvent Extr. Ion Exch.* **1990**, *8*, 759−781.

(23) Leoncini, A.; Huskens, J.; Verboom, W. Ligands for F-Element Extraction Used in the Nuclear Fuel Cycle. *Chem. Soc. Rev.* **2017**, *46*, 7229−7273.

(24) Nilsson, M.; Nash, K. L. A Review of the Development and Operational Characteristics of the TALSPEAK Process. *Solvent Extr. Ion Exch.* **2007**, *25*, 665−701.

(25) Nash, K. L. The Chemistry of TALSPEAK: A Review of the Science. *Solvent Extr. Ion Exch.* **2015**, *33*, 1−55.

(26) Martell, A. E.; Smith, R. M. *Critical Stability Constants*; Plenum Press: New York, 1974; Vol. *1*.
(27) Chang, C. A.; Rowland, M. E. Metal Complex Formation with 1,10-Diaza-4,7,13,16-Tetraoxacyclooctadecane-N, N'-Diacetic Acid. An Approach to Potential Lanthanide Ion Selective Reagents. *Inorg. Chem.* **1983**, *22*, 3866−3869.
(28) Hancock, R. D.; Bhavan, R.; Shaikjee, M. S.; Wade, P. W.; Hearn, A. The Metal Ion Size-Dependent Pattern of Stabilization Produced by Adding Alcoholic or Ethereal Oxygen Donors to Ligands. *Inorg. Chim. Acta* **1986**, *112*, L23−L25.
(29) Damu, K. V.; Shaikjee, M. S.; Michael, J. P.; Howard, A. S.; Hancock, R. D. Control of Metal Ion Selectivity in Ligands Containing Neutral Oxygen and Pyridyl Groups. *Inorg. Chem.* **1986**, *25*, 3879−3883.
(30) Hancock, R. D.; Bhavan, R.; Wade, P. W.; Boeyens, J. C. A.; Dobson, S. M. Ligand Design for Complexation in Aqueous Solution. 1. Neutral Oxygen Donor Bearing Groups as a Means of Controlling Size-Based Selectivity for Metal Ions. *Inorg. Chem.* **1989**, *28*, 187−194.
(31) Hancock, R. D.; Martell, A. E. Ligand Design for Selective Complexation of Metal Ions in Aqueous Solution. *Chem. Rev.* **1989**, *89*, 1875−1914.
(32) Brücher, E.; Györi, B.; Emri, J.; Solymosi, P.; Sztanyik, L. B.; Varga, L. 1,10-Diaza-4,7,13,16-Tetraoxacyclooctadecane-1,10-Bis-(Malonate), a Ligand with High Sr^{2+}/Ca^{2+} and Pb^{2+}/Zn^{2+} Selectivities in Aqueous Solution. *J. Chem. Soc., Chem. Commun.* **1993**, 574−575.
(33) Regueiro-Figueroa, M.; Barriada, J. L.; Pallier, A.; Esteban-Gómez, D.; de Blas, A.; Rodríguez-Blas, T.; Tóth, É.; Platas-Iglesias, C. Stabilizing Divalent Europium in Aqueous Solution Using Size-Discrimination and Electrostatic Effects. *Inorg. Chem.* **2015**, *54*, 4940−4952.
(34) Roca-Sabio, A.; Mato-Iglesias, M.; Esteban-Gómez, D.; Toth, É.; de Blas, A.; Platas-Iglesias, C.; Rodríguez-Blas, T. Macrocyclic Receptor Exhibiting Unprecedented Selectivity for Light Lanthanides. *J. Am. Chem. Soc.* **2009**, *131*, 3331−3341.
(35) Ferreirós-Martínez, R.; Esteban-Gómez, D.; Tóth, É.; de Blas, A.; Platas-Iglesias, C.; Rodríguez-Blas, T. Macrocyclic Receptor Showing Extremely High Sr(II)/Ca(II) and Pb(II)/Ca(II) Selectivities with Potential Application in Chelation Treatment of Metal Intoxication. *Inorg. Chem.* **2011**, *50*, 3772−3784.
(36) Jensen, M. P.; Chiarizia, R.; Shkrob, I. A.; Ulicki, J. S.; Spindler, B. D.; Murphy, D. J.; Hossain, M.; Roca-Sabio, A.; Platas-Iglesias, C.; de Blas, A.; Rodríguez-Blas, T. Aqueous Complexes for Efficient Size-Based Separation of Americium from Curium. *Inorg. Chem.* **2014**, *53*, 6003−6012.
(37) Jensen, M. P.; Chiarizia, R.; Ulicki, J. S.; Spindler, B. D.; Murphy, D. J.; Hossain, M. M.; Roca-Sabio, A.; de Blas, A.; Rodríguez-Blas, T. Solvent Extraction Separation of Trivalent Americium from Curium and the Lanthanides. *Solvent Extr. Ion Exch.* **2015**, *33*, 329−345.
(38) Thiele, N. A.; Brown, V.; Kelly, J. M.; Amor-Coarasa, A.; Jermilova, U.; MacMillan, S. N.; Nikolopoulou, A.; Ponnala, S.; Ramogida, C. F.; Robertson, A. K. H.; Rodríguez-Rodríguez, C.; Schaffer, P.; Williams, C., Jr.; Babich, J. W.; Radchenko, V.; Wilson, J. J. An Eighteen-Membered Macrocyclic Ligand for Actinium-225 Targeted Alpha Therapy. *Angew. Chem., Int. Ed.* **2017**, *56*, 14712−14717.
(39) Thiele, N. A.; MacMillan, S. N.; Wilson, J. J. Rapid Dissolution of $BaSO_4$ by Macropa, an 18-Membered Macrocycle with High Affinity for Ba^{2+}. *J. Am. Chem. Soc.* **2018**, *140*, 17071−17078.
(40) Thiele, N. A.; Woods, J. J.; Wilson, J. J. Implementing f-Block Metal Ions in Medicine: Tuning the Size Selectivity of Expanded Macrocycles. *Inorg. Chem.* **2019**, *58*, 10483−10500.
(41) Kelly, J. M.; Amor-Coarasa, A.; Ponnala, S.; Nikolopoulou, A.; Williams, C., Jr.; Thiele, N. A.; Schlyer, D.; Wilson, J. J.; DiMagno, S. G.; Babich, J. W. A Single Dose of ^{225}Ac-RPS-074 Induces a Complete Tumor Response in a LNCaP Xenograft Model. *J. Nucl. Med.* **2019**, *60*, 649−655.
(42) Aluicio-Sarduy, E.; Thiele, N. A.; Martin, K. E.; Vaughn, B. A.; Devaraj, J.; Olson, A. P.; Barnhart, T. E.; Wilson, J. J.; Boros, E.; Engle, J. W. Establishing Radiolanthanum Chemistry for Targeted Nuclear Medicine Applications. *Chem. - Eur. J.* **2020**, *26*, 1238−1242.
(43) Walton, J. W.; Bari, L. D.; Parker, D.; Pescitelli, G.; Puschmann, H.; Yufit, D. S. Structure, Resolution and Chiroptical Analysis of Stable Lanthanide Complexes of a Pyridylphenylphosphinate Triazacyclononane Ligand. *Chem. Commun.* **2011**, *47*, 12289−12291.
(44) Walton, J. W.; Carr, R.; Evans, N. H.; Funk, A. M.; Kenwright, A. M.; Parker, D.; Yufit, D. S.; Botta, M.; De Pinto, S.; Wong, K.-L. Isostructural Series of Nine-Coordinate Chiral Lanthanide Complexes Based on Triazacyclononane. *Inorg. Chem.* **2012**, *51*, 8042−8056.
(45) Polášek, M.; Šedinová, M.; Kotek, J.; Vander Elst, L.; Muller, R. N.; Hermann, P.; Lukeš, I. Pyridine-*N*-Oxide Analogues of DOTA and Their Gadolinium(III) Complexes Endowed with a Fast Water Exchange on the Square-Antiprismatic Isomer. *Inorg. Chem.* **2009**, *48*, 455−465.
(46) Lee, S. J.; Kim, H. S.; Yang, H. W.; Yoo, B. W.; Yoon, C. M. Synthesis of Diethyl Pyridin-2-ylphosphonates and Quinolin-2-ylphosphonates by Deoxygenative Phosphorylation of the Corresponding *N*-Oxides. *Bull. Korean Chem. Soc.* **2014**, *35*, 2155−2158.
(47) Salaam, J.; Tabti, L.; Bahamyirou, S.; Lecointre, A.; Hernandez Alba, O.; Jeannin, O.; Camerel, F.; Cianférani, S.; Bentouhami, E.; Nonat, A. M.; Charbonnière, L. J. Formation of Mono- and Polynuclear Luminescent Lanthanide Complexes Based on the Coordination of Preorganized Phosphonated Pyridines. *Inorg. Chem.* **2018**, *57*, 6095−6106.
(48) Bernier, D.; Wefelscheid, U. K.; Woodward, S. Properties, Preparation and Synthetic Uses of Amine *N*-Oxides. An Update. *Org. Prep. Proced. Int.* **2009**, *41*, 173−210.
(49) Jensen, K. A. Tentative Proposals for Nomenclature of Absolute Configurations Concerned with Six-Coordinated Complexes Based on the Octahedron. *Inorg. Chem.* **1970**, *9*, 1−5.
(50) Rohovec, J.; Lukeš, I.; Vojtíšek, P.; Císařová, I.; Hermann, P. Complexing Properties of Phosphinic Analogues of Glycine. *J. Chem. Soc., Dalton Trans.* **1996**, 2685−2691.
(51) Weaver, B.; Kappelmann, F. A. Preferential Extraction of Lanthanides over Trivalent Actinides by Monoacidic Organophosphates from Carboxylic Acids and from Mixtures of Carboxylic and Aminopolyacetic Acids. *J. Inorg. Nucl. Chem.* **1968**, *30*, 263−272.

https://dx.doi.org/10.1021/acs.inorgchem.0c02413
Inorg. Chem. 2020, 59, 16522−16530